18th International Conference on Information Fusion
Washington, DC - July 6-9, 2015

Joint Multi-Bernoulli RFS for Two-target Scenario

Suqi Li*, Wei Yi*, Mark R. Morelande†, Bailu Wang*, Lingjiang Kong*
*University of Electronic Science and Technology of China, School of Electronic Engineering, Chengdu City, China,
Email: {kussoyi, lingjiang.kong}@gmail.com
†RMIT University, Australia, Email: m.morelande@gmail.com

***Abstract*—In this paper, we propose a new class of random finite set (RFS), which is the union of a group of Bernoulli RFSs with unknown level of correlation, whose statistics are considered jointly. The proposed RFS is referred to as joint multi-Bernoulli (JMB) RFS defined by a set of parameters. As a preliminary study, this paper provides the derivations of set density, set marginal density of JMB RFS family, and the resultant tracking filter for a two-target scenario based on finite-set statistics (FISST). Note that the theoretically sound way of computing the set marginal density is not well defined in current FISST. The JMB RFS family offers a parameterized and generalized set density which bridges the gap between set density and vector density. Hence, the JMB RFS family inherits several advantages of vector density, such as analyzing the correlation between states, extracting the statistics of partial states from global statistics conveniently, and embedding the target identities implicitly. The corresponding tracking filter has an accurate update equations with no need to specify measurement model, and can be further improved by utilizing the advantages of JMB RFS family. The aforementioned advantages are clearly highlighted by the numerical results.**

I. Introduction

Multi-target tracking system usually involves simultaneously estimating the states, and the number of targets moving in a surveillance area. Moreover, the number of target is usually unknown and time-varying due to births and deaths of targets. In traditional multi-target tracking, e.g., joint probabilistic data association (JPDA) [1], multi-hypotheses tracker [2], [3] and multi-target particle filter [4]–[7], individual target states are usually stacked into a vector formed multi-target state whose statistics is described by a joint vector density. The fully developed probability theory owns many useful statistical tools which offer more freedom for development of vector based multi-target tracking. For example, for a vector formed multi-target state, it is convenient to analyze the correlation between states by computing correlation coefficient and extract the statistics of partial target states by computing the marginal densities of the corresponding sub-vectors, and many scholars have develop improvement strategies utilizing these tools, e.g., the adaptive parallel filtering according to the correlation between targets, to enhance the tracking performance and reduce the computation burden [6]–[8]. However, vector density can only depict the statistics of a fixed number of targets theoretically as the dimensionality of vector is fixed. As a result, the vector based multi-target tracking usually needs an additional process to accommodate births and deaths of targets.

Recently, multi-target tracking approaches in the random finite set (RFS) framework [9]–[24] represent the collection of multiple states as a finite set. The RFS, whose cardinality and individual states are both random, is much more matching the system of multi-target tracking. In order to handle the statistics of finite sets, Mahler developed powerful and practical mathematical tools, referred to as finite set statistics (FISST) [9]–[11], which also provides a systematic, unified approach for multi-target tracking based on explicit, comprehensive, unified statistical models of multi-target systems. The centerpiece of the RFS approach is the optimal Bayesian multi-target filter, but it always involves set integral making it computationally intractable. In order to alleviate the numerical complexity, several approximate methods, i.e., Probability hypothesis density (PHD)/cardinalized PHD (CPHD) [12]–[14], multi-Bernoulli filters [15]–[17] in which posterior or prior are approximated as poisson, independent, identically distributed (i.i.d.) clutter or Multi-Bernoulli processes [9], were proposed. These processes assuming independence between target states dramatically reduce the computation burden, but lose precision with highly approximate update equations. Later, Ba-Ngu Vo *et al.* relaxed the independence assumption, and proposed GLMB process [18]–[24], which admits correlation between target states and obtains an accurate closed form update equations for the standard measurement model. However, as it still assumes independence under different hypotheses, GLMB process cannot obtain accurate update equations for the nonstandard measurement models.

In this paper, we propose a new class of RFS, which is the union of a group of Bernoulli RFSs whose statistics are considered jointly, and thus is referred to as joint multi-Bernoulli (JMB) RFS. As the results of preliminary study, this paper provides the derivations of the set density, marginal set density of JMB RFS, and the resultant tracking filter for a two-target scenario. The study on two-target scenario is meaningful for it is sufficient to reflect the advantages of the JMB RFS family and lays the foundation of multi-target scenario. It should be remarked that the theoretically sound way of computing the set marginal density is not well defined in current FISST, but is provided in this paper. The JMB RFS whose maximum cardinality is 2, is called as JMB-2 RFS.

The JMB-2 RFS family provides a generalized set density which can accommodate unknown level of correlation between target states, and thus the relevant tracking filter, JMB-2

This work was supported by the National Natural Science Foundation of China (61201276, 61178068 and 61301266), Fundamental Research Funds of Central Universities (ZYGX2012Z001, ZYGX2013J012), Chinese Post-doctoral Science Foundation (2014M550465) and Program for New Century Excellent Talents in University (A1098524023901001063).

filter can obtain an accurate closed form update equation for any kind of measurement model. A JMB-2 RFS is completely determined by a set of parameters which consist of the probabilities of different hypotheses and vector densities conditioned on different hypotheses. Different hypotheses here indicate the existence of different targets. Hence, The JMB-2 RFS inherits some advantages of vector density by utilizing mature statistical tools for random vectors. The advantages of JMB-2 RFS, in turn, offer the potential and freedom for the development and improvement of JMB-2 filter.

Firstly, the correlation between states in a JMB-2 RFS can be analyzed conveniently by computing the correlation coefficient about targets existence, and the mutual correlation coefficient matrix [26] under hypothesis where both targets exist.

Secondly, the JMB-2 RFS enjoys a congenital advantage to extract the statistics of partial states from the global statistics of multi-target state by computing the set marginal density.

Thirdly, the identities of target states are implicitly embedded with no need to augment target state with an extra label.

II. Notations and Three Statistical Descriptors

A. Notations

We adhere to the convention that single-target states are represented by lowercase letters, e.g., $\mathbf{x}$, while multi-target states are represented by uppercase letters, e.g., $\mathbf{X}$, X. Symbols for vector formed states and their densities are bolded, e.g., $\mathbf{x}$, $\mathbf{X}$, $\mathbf{f}(\mathbf{X})$, while symbols for set formed states and their densities are italic, e.g., X,$\overline{X}$, $f(X)$. To distinguish labelled states and distributions from the unlabelled ones, letters with a line on the top are adopted for the labelled ones, e.g., $\overline{\mathbf{x}}$, $\overline{X}$, $\overline{f}(\overline{X})$. Moreover, blackboard bold letters represent spaces, e.g., the state space is represented by $\mathbb{X}$, the label space by $\mathcal{F}(\mathbb{X})$, and the observation space by $\mathbb{Z}$. The collection of all finite sets of $\mathbb{X}$ is denoted by $\mathcal{F}(\mathbb{X})$. The joint probability density function, integration and derivative for a random vector are based on the Euclidean notion of density, integration and derivative, and are named as vector density, vector integration, vector derivative, respectively. The multi-target probability density, integration and derivative for an RFS are based on FISST notion of density, integration and derivative, and are named as set density, integration and derivative, respectively.

The labelled single target state $\mathbf{x}$ is constructed by augmenting a state $\mathbf{x} \in \mathbb{X}$ with a label $\ell \in \mathbb{L}$. The labels are usually drawn from a discrete label space, $\mathbb{L} = \{\alpha_i, i \in \mathbb{N}\}$, where all α_i are distinct and the index space $\mathbb{N}$ is the set of positive integers. For convenience, in this paper, we use $\mathbb{N}$ as the the label space, i.e., $\mathbb{L} = \mathbb{N}$.

To admit arbitrary arguments like sets, vectors and integers, the generalized Kronecker delta function is given by

$$\delta_Y(X) \triangleq \begin{cases} 1, \text{if} X = Y \\ 0, \text{otherwise} \end{cases} \tag{1}$$

The vector integrals are using the inner product notation. For functions $\mathbf{a}(\mathbf{x})$ and $\mathbf{b}(\mathbf{x})$ defined on $\mathbb{X}$, the inner product is represented as $\langle \mathbf{a}, \mathbf{b} \rangle_1 = \int_{\mathbb{X}} \mathbf{a}(\mathbf{x})\mathbf{b}(\mathbf{x}) d\mathbf{x}$. For functions $\mathbf{c}(\mathbf{x}_1, \mathbf{x}_2)$ and $\mathbf{e}(\mathbf{x}_1, \mathbf{x}_2)$ defined on $\mathbb{X}^2$, the inner product is represented as $\langle \mathbf{c}, \mathbf{e} \rangle_2 = \int_{\mathbb{X}^2} \mathbf{c}(\mathbf{x}_1, \mathbf{x}_2)\mathbf{e}(\mathbf{x}_1, \mathbf{x}_2) d(\mathbf{x}_1, \mathbf{x}_2)$. For some special cases, the inner productions also are denoted as $\langle \mathbf{a}(\cdot), \mathbf{b}(\cdot) \rangle_1$ and $\langle \mathbf{c}(\cdot, \star), \mathbf{e}(\cdot, \star) \rangle_2$, where $\cdot$ and $\star$ are used to distinguish different dimensions.

B. Three Statistical Descriptors for Multi-target State

In this subsection, we compare three statistical descriptors for multi-target state with respect to two definitely existing targets $\mathbf{x}_1, \mathbf{x}_2 \in \mathbb{X}$. The total target number is fixed to 2, and $\mathbb{L} = \{1, 2\}$ denote the target label space.

• Unlabelled set density: the multi-target state is represented by the unlabelled finite set $X = \{\mathbf{x}_1, \mathbf{x}_2\}$ whose statistics is characterized by set density $f(X) = f(\{\mathbf{x}_1, \mathbf{x}_2\})$ in FISST framework.

• Vector density: the multi-target state is represented by the vector $\mathbf{X} = (\mathbf{x}_1, \mathbf{x}_2)$ which is constructed by stacking individual target states. The statistics of $\mathbf{X}$ is characterized by vector density [1]–[8], [26], $\mathbf{f}(\mathbf{X}) = \mathbf{f}((\mathbf{x}_1, \mathbf{x}_2))$.

• Labelled set density: the multi-target state is represented by labelled finite set $\overline{X} = \{(\mathbf{x}_1, \ell_1), (\mathbf{x}_2, \ell_2)\}$ whose statistics is characterized by the labelled set density $\overline{f}(\overline{X}) = \overline{f}(\{(\mathbf{x}_1, \ell_1), (\mathbf{x}_2, \ell_2)\})$ [18], [19], where $\ell_i \in \mathbb{L}$ denote the target label of $\mathbf{x}_i$, $i = 1, 2$.

Then, we discuss the relationship and the relative merits between these three statistical descriptors.

• The relationship between vector density $\mathbf{f}(\mathbf{X})$ and unlabelled set density $f(X)$ can be represented as [27], [28]:

$$f(\{\mathbf{x}_1, \mathbf{x}_2\}) = \mathbf{f}((\mathbf{x}_1, \mathbf{x}_2)) + \mathbf{f}((\mathbf{x}_2, \mathbf{x}_1)) \tag{2}$$

On one hand, for the vector formed multi-target state, the order implicit in the components of a vector implies that targets are labelled. Target labels can reflected from the ordered vector density, i.e., $\mathbf{f}((\mathbf{x}_1, \mathbf{x}_2)) \neq \mathbf{f}((\mathbf{x}_2, \mathbf{x}_1))$. (2) indicates that the transformation from vector density to unlabelled set density can be seen as a process of information compression. During this process, target label information is lost, and it is the target states that only matter. Thus we have $f(\{\mathbf{x}_1, \mathbf{x}_2\}) = f(\{\mathbf{x}_2, \mathbf{x}_1\})$.

It has been pointed out in [27] that as for a given set density, there exist a family of vector densities corresponding with it. Based on [27], the RFS family of $\mathbf{f}((\mathbf{x}_1, \mathbf{x}_2))$ is defined as:

$$\begin{aligned} \mathcal{R}_{\mathbf{f}(\mathbf{X})} = \{\acute{\mathbf{f}}(\mathbf{X}) : \acute{\mathbf{f}}((\mathbf{x}_1, \mathbf{x}_2)) + \acute{\mathbf{f}}((\mathbf{x}_2, \mathbf{x}_1)) \\ = \mathbf{f}((\mathbf{x}_1, \mathbf{x}_2)) + \mathbf{f}((\mathbf{x}_2, \mathbf{x}_1))\} \end{aligned} \tag{3}$$

Importantly, some vector densities within the RFS family, which are less multi-modal, are more convenient to approximate than others.

On the other hand, for the vector formed multi-target state, the correlation between target states can be analyzed, and the statistics of partial states can be extracted, conveniently, by utilizing the mature statistical tool for random vector [26]. The correlation between $\mathbf{x}_1$ and $\mathbf{x}_2$ can be analyzed by utilizing the joint vector density $\mathbf{f}((\mathbf{x}_1, \mathbf{x}_2))$ through computing the mutual correlation coefficient matrix [26], but is difficult to be analyzed by using the set density $f(\{\mathbf{x}_1, \mathbf{x}_2\})$ for the existing

FISST lacks the theoretical method to analyze the correlation. We also can obtain the statistics of $\mathbf{x}_1$ or $\mathbf{x}_2$ from the big random vector $(\mathbf{x}_1, \mathbf{x}_2)$ by computing the vector marginal density of $\mathbf{x}_1$ or $\mathbf{x}_2$, e.g., $\int_{\mathbb{X}} \mathbf{f}((\mathbf{x}_1, \mathbf{x}_2))d\mathbf{x}_2$, but it is difficult to obtain the statistics of the sub-set $\{\mathbf{x}_1\}$ from the big RFS $\{\mathbf{x}_1, \mathbf{x}_2\}$, for the marginal density for a sub-set is not well defined in FISST.

• The labelled RFS is first proposed in [18] which provides procedures for generating special labelled RFSs, such as the labelled Poisson RFS, and the labelled multi-Bernoulli RFS, etc. Here, we present a procedure for generating an ordinary labelled RFS with cardinality fixed to 2, shown in Table I. The likelihood (probability density) that the procedure in Table I generates the points in that order $(\mathbf{x}_1, \ell_1), (\mathbf{x}_2, \ell_2)$ can be represented as:

Thus the labelled density which characterizes the labelled RFS generated by the procedure in Table I is the symmetrization of $\overline{\mathbf{L}}(((\mathbf{x}_1, \ell_1), (\mathbf{x}_2, \ell_2)))$ over all permutations of {1,2}, i.e.,

$$\begin{aligned} &\overline{f}\{(\mathbf{x}_1, \ell_1), (\mathbf{x}_2, \ell_2)\} = \\ &\delta_{(1,2)}((\ell_1,\ell_2))\mathbf{f}((\mathbf{x}_1, \mathbf{x}_2))+\delta_{(1,2)}((\ell_2,\ell_1))\mathbf{f}((\mathbf{x}_2,\mathbf{x}_1)) \end{aligned} \tag{4}$$

$$\overline{\mathbf{L}}(((\mathbf{x}_1, \ell_1), (\mathbf{x}_2, \ell_2))) = \delta_{(1,2)}((\ell_1, \ell_2))\mathbf{f}((\mathbf{x}_1, \mathbf{x}_2)) \tag{5}$$

TABLE I
THE PROCEDURE OF GENERATING A LABELLED RFS WITH CARDINALITY FIXED TO 2

Sampling a Labelled RFS
Initialize $\overline{X} = \emptyset$
Sample $(\mathbf{x}_1, \mathbf{x}_2) \sim \mathbf{f}((\mathbf{x}_1, \mathbf{x}_2))$
for i=1:2
$\overline{X} = \overline{X} \cup \{(\mathbf{x}_i, i)\}$
end

The relationship between the vector density $\mathbf{f}(\mathbf{X})$ and the labelled set density $\overline{f}(\overline{X})$ can exploited from (4). The sum in (4) is zero, except for the case $\{\ell_1, \ell_2\} = \{1, 2\}$ where $(\ell_1, \ell_2) = (1, 2)$ or $(\ell_2, \ell_1) = (1, 2)$. Thus, for (4), only one sum-item works. From this point, the labelled set density is equivalent to the vector density. This conclusion also has been proved in [28]. Even though the labelled set density incorporates target label information, it is also hard to extract statistics of partial states confined by existing FISST.

In terms of aspects discussed above, vector density is the best descriptor for definitely existing targets among these three approaches. The vector density owns more complete information, especially the target label information. Moreover, in the vector notation, it is convenient to analyze the correlation between target states and extract the statistics of partial target states.

III. JMB-2 RFS

In practical scenarios, the number of existing targets is usually unknown and time-varying. The reason is that apart from the uncertainty about target kinematics, there is still uncertainty about whether targets exist or not. For instance, targets may appear or die, and targets may be submerged by heavy clutter. Here, we call a target which may or may not exist as a "twinkling" target. It is reasonable to model a group of unknown and time-varying number of targets as a fixed number of "twinkling" targets, for example a multi-Bernoulli RFS. Though vector density is the best statistics descriptor for two definitely existing targets in terms of these aspects discussed in subsection II-B, it cannot describe the complicated statistics of "twinkling" targets in a theoretically sound way for the dimension of a random vector is fixed. Hence, we resort to the RFS framework.

A. Definition of JMB-2 RFS

Consider two "twinkling" targets. Each single "twinkling" target is naturally modelled as a Bernoulli RFS ψ_i whose cardinality only has two possible values (0 or 1) such that $\psi_i = \emptyset$ when target i does not exist, and $\psi_i = \{\mathbf{x}_i\}$ when target i dose exist, where the index of ψ_i, $i = 1, 2$ has the function to distinguish target identities and thus is served as the target label, $\mathbf{x}_i \in \mathbb{X}$ denotes the kinematical state of target i conditioned on existence, and $\mathbb{X}$ is the single target space. The two "twinkling" targets are mathematically modelled as the union $\Psi = \psi_1 \cup \psi_2$, and the correlation between ψ_1 and ψ_2 is completely unknown. Sometimes the two targets are far enough apart that their randomness is independent of each other. Sometimes, the two targets are so close together that their observability is affected by the same underlying noise and clutter, thus their sensing situation being observed will have correlation. Hence, it is unreasonable to assume ψ_1 and ψ_2 statistically independent, as a multi-Bernoulli RFS does. A joint distribution is appropriate to describe the uncertainty of two targets' existence. We define a random vector (E_1, E_2), where

$$E_i = \begin{cases} 1, & \psi_i \neq \emptyset \\ 0, & \psi_i = \emptyset \end{cases}, i = 1, 2$$

and the joint distribution of (E_1, E_2) is

$$\Pr\{E_1 = j, E_2 = k\} = \epsilon_{jk}, \quad (j, k = 0, 1) \tag{6}$$

We use an idiomatic table shown in Table II to denote the joint distribution of (E_1, E_2).

TABLE II
THE JOINT DISTRIBUTION OF (E_1, E_2)

E_2 \ E_1	0	1
0	ϵ_{00}	ϵ_{10}
1	ϵ_{01}	ϵ_{11}

Based on the definition of the correlation coefficient [26], the correlation coefficient between E_1 and E_2 can be computed as:

$$\rho_{E_1E_2} = \frac{\epsilon_{11} - (\epsilon_{10} + \epsilon_{11})(\epsilon_{01} + \epsilon_{11})}{\sqrt{(\epsilon_{10} + \epsilon_{11})(1 - \epsilon_{10} - \epsilon_{11})(\epsilon_{01} + \epsilon_{11})(1 - \epsilon_{01} - \epsilon_{11})}} \tag{7}$$

Then a multi-hypotheses organized stochastic model is adopted to describe the statistics of Ψ. The different values of (E_1, E_2) are considered as different hypotheses which are shown as:

- H_{00}: $(E_1, E_2) = (0, 0)$, which means neither of two targets exist, and under this hypothesis $\Psi = \psi_1 \cup \psi_2 = \emptyset$.
- H_{10}: $(E_1, E_2) = (1, 0)$, which means target 1 exists, $\psi_1 = \{\mathbf{x}_1\}$ and target 2 does not exist, $\psi_2 = \emptyset$. Under this Hypothesis, $\Psi = \psi_1 \cup \psi_2 = \{\mathbf{x}_1\}$ and the probability density of $\mathbf{x}_1$ is $\boldsymbol{\varrho}_{10}(\mathbf{x}_1)$.
- H_{01}: $(E_1, E_2) = (0, 1)$, which means target 2 exists, $\Psi = \{\mathbf{x}_2\}$ and target 1 does not exist, $\Psi = \emptyset$. Under this Hypothesis, $\Psi = \psi_1 \cup \psi_2 = \{\mathbf{x}_2\}$ and the probability density of $\mathbf{x}_2$ is $\boldsymbol{\varrho}_{01}(\mathbf{x}_2)$.
- H_{11}: $(E_1, E_2) = (1, 1)$, which means both target 1 and target 2 exist, i.e., $\psi_1 = \{\mathbf{x}_1\}$ and $\psi_2 = \{\mathbf{x}_2\}$. Under this hypothesis, $\Psi = \psi_1 \cup \psi_2 = \{\mathbf{x}_1, \mathbf{x}_2\}$. The statistics of the ordered vector $(\mathbf{x}_1, \mathbf{x}_2) \in \mathbb{X}^2$ is depicted by vector density $\boldsymbol{\varrho}_{11}((\mathbf{x}_1, \mathbf{x}_2))$.

Under hypothesis H_{11}, where both targets exist, the correlation between the states $\mathbf{x}_1$ and $\mathbf{x}_2$ can be analyzed by computing the mutual correlation coefficient matrix [26] based on the vector density $\boldsymbol{\varrho}_{11}((\mathbf{x}_1, \mathbf{x}_2))$, and is denoted as $\boldsymbol{\rho}_{\mathbf{x}_1\mathbf{x}_2|H_{11}}$.

Remark: Under hypothesis H_{11}, we should have adopted the set density in order to describe the statistics of Ψ, however, based on the discussions in the subsection II-B, vector density is better than set density in terms of its convenience in analyzing the correlation, extracting the statistics of partial target states and incorporation of target labels. More importantly a set density can be completely characterized by a vector density in the RFS family corresponding to this set density [27]. Thus, under hypothesis H_{11}, we choose a less multi-modal vector density [27], [28] $\boldsymbol{\varrho}_{11}((\mathbf{x}_1, \mathbf{x}_2))$ within the RFS family of the set density of Ψ, and the order implicit in components of $\boldsymbol{\varrho}_{11}((\mathbf{x}_1, \mathbf{x}_2))$ is consistent with the order of indexes of Ψ_1 and Ψ_2.

Overall, Ψ is the union of two Bernoulli RFSs $\psi_i, i = 1, 2$ with unknown level of correlation whose statistics are considered jointly, and thus is referred to as joint multi-Bernoulli-2 (JMB-2) RFS where 2 indicates two "twinkling" targets are involved. A JMB-2 RFS can be completely defined by a set of parameters $\{\epsilon_{10}, \boldsymbol{\varrho}_{10}, \epsilon_{01}, \boldsymbol{\varrho}_{01}, \epsilon_{11}, \boldsymbol{\varrho}_{11}\}$, referred to as JMB-2 parameters. The parameter ϵ_{00} is omitted, for it can be determined by $\epsilon_{00} = 1 - \epsilon_{10} - \epsilon_{01} - \epsilon_{11}$. The JMB-2 parameters include probabilities of different hypotheses and the vector densities of target states under different hypotheses. Different hypotheses mean the existences of different targets. All hypotheses consider uncertainty of target existence jointly and under the hypothesis where both targets exist, the statistics of two target states are considered jointly. Also the correlation between ψ_1 and ψ_2 can be analyzed from two levels: a) computing the correlation coefficient between E_1 and E_2, i.e., $\rho_{E_1E_2}$; b) computing the mutual correlation coefficient matrix under hypothesis where both targets exist, $\boldsymbol{\rho}_{\mathbf{x}_1\mathbf{x}_2|H_{11}}$.

Remark: The JMB-2 RFS can be generalized to the JMB-N ($N > 2$) RFS to describe the statistics of more than two "twinkling" targets, which will be studied in the future. The JMB-2 RFS also can be degenerated to JMB-1 RFS which only describes the single "twinkling" target. Obviously, a JMB-1 RFS is a Bernoulli RFS which is completely determined by Bernoulli parameters $\{r, \mathbf{p}(\mathbf{x})\}$ with r the probability of existence and $\mathbf{p}(\mathbf{x})$ the density conditioned on existence.

B. Set Density of JMB-2 RFS

The following results show the set density and the cardinality distribution of JMB-2 RFS.

Proposition 1: If Ψ is a JMB-2 RFS defined by its JMB-2 parameters $\{\epsilon_{10},\boldsymbol{\varrho}_{10},\epsilon_{01},\boldsymbol{\varrho}_{01},\epsilon_{11},\boldsymbol{\varrho}_{11}\}$, the set density of Ψ is

$$f_\Psi(X) = \begin{cases} \epsilon_{00}, & X = \emptyset \\ \epsilon_{10}\boldsymbol{\varrho}_{10}(\mathbf{x}) + \epsilon_{01}\boldsymbol{\varrho}_{01}(\mathbf{x}), & X = \{\mathbf{x}\} \\ \epsilon_{11}[\boldsymbol{\varrho}_{11}((\mathbf{x}_1, \mathbf{x}_2)) + \boldsymbol{\varrho}_{11}((\mathbf{x}_2, \mathbf{x}_1))], & X = \{\mathbf{x}_1, \mathbf{x}_2\} \\ 0, & |X| \geq 3 \end{cases} \tag{8}$$

Proof: Because of the multi-hypotheses structure of Ψ, we can utilize the whole probability formula [26] to represent the belief mass function [9] of Ψ ,

$$\begin{aligned} \beta_\Psi(S) &= \Pr(\Psi \subseteq S) = \Pr(\psi_1 \subseteq S, \psi_2 \subseteq S) \\ &+ \epsilon_{01} \Pr(\mathbf{x}_2 \in S | E_1 = 0, E_2 = 1) \\ &+ \epsilon_{11} \Pr(\mathbf{x}_1 \in S, \mathbf{x}_2 \in S | E_1 = 1, E_2 = 1) \end{aligned} \tag{9}$$

with $S \subseteq \mathbb{X}$ the observation region. Note that the last term in sum of (9) is further represented as:

$$\begin{aligned} &\Pr(\mathbf{x}_1 \in S, \mathbf{x}_2 \in S | E_1 = 1, E_2 = 1) \\ &\qquad = \Pr((\mathbf{x}_1, \mathbf{x}_2) \in S \times S | E_1 = 1, E_2 = 1) \end{aligned}$$

Using JMB-2 parameters of Ψ, (9) can be further represented as

$$\begin{aligned} \beta_\Psi(S) = \epsilon_{00} + \epsilon_{10} \int_S \boldsymbol{\varrho}_{10}(\mathbf{x}_1) d\mathbf{x}_1 + \epsilon_{01} \int_S \boldsymbol{\varrho}_{01}(\mathbf{x}_2) d\mathbf{x}_2 \\ + \epsilon_{11} \int_{S \times S} \boldsymbol{\varrho}_{11}((\mathbf{x}_1, \mathbf{x}_2)) d(\mathbf{x}_1, \mathbf{x}_2) \end{aligned} \tag{10}$$

It follows from Radon-Nikodým theorem [9] that set density of Ψ can be constructed by taking the set derivation of the belief-mass function of Ψ:

$$f_\Psi(X) = \frac{\delta \beta_\Psi}{\delta X}(\emptyset) \tag{11}$$

Substituting (10) into (11), the set density of Ψ can be obtained.

Remark: In the the remainder of this paper, the item JMB-2 density is used to mean the set density of a JMB-2 RFS. The JMB-2 density of form (8) provides a unified representation of statistics of two "twinkling" targets and is the basis of tracking relevant filter.

C. Set Marginal Density of JMB-2 RFS

For vector formed multi-target state, partial target states can be represented as a sub-vector and the well-defined vector marginal density [26] in Euclidean notion of integration is a useful tool for extracting statistics of sub-vector from global statistics. For set formed multi-target state, partial target states are represented as a subset. However, in FISST, the marginal density for random sub-set is not well-defined. It is difficult to exact statistics of sub-set from global set density in a theoretically sound way. We note that, in FISST, many concepts relevant to RFS are the natural generalization of the corresponding concepts of random vector. For instance, the belief-mass function and the set density are respectively natural generalizations of the probability-mass function and the vector density [9], respectively. Motivated by this, in this subsection, we give a rational definition of set marginal density by the natural generalization of the vector marginal density.

Definition 1: Let Ψ be an RFS. Then for any random finite subset of Ψ, denoted by ψ, its set density function $f_\psi(X)$, is called set marginal density of ψ with respect to Ψ.

Proposition 2: Let Ψ be an RFS. Then for any random finite subset of Ψ, denoted by ψ, its set marginal density of ψ with respect to Ψ, denoted by $f_\psi(X)$ can be derived by

$$f_\psi(X) = \left.\frac{\delta \Pr(\psi \subseteq S, \Psi/\psi \subseteq \mathbb{X})}{\delta X}\right|_{S=\emptyset} \tag{12}$$

where "$\delta/\delta X$" denotes a set derivative [9].

Note that our goal is to compute the set marginal density $f_\psi(X)$ from the global set density $f_\Psi(\mathbf{X})$. A direct idea is to represent the probability $\Pr(\psi \subseteq S, \Psi/\psi \subseteq \mathbb{X})$ in (12) as the set integral of $f_\Psi(\mathbf{X})$ and then take set derivative. However, $\Pr(\psi \subseteq S, \Psi/\psi \subseteq \mathbb{X})$ denotes the probability that the elements in Ψ belong to different spaces such that it cannot be represented as the set integral of $f_\Psi(\mathbf{X})$ based on the definition of set integral [9]. Hence, though *Proposition 2* gives a fundamental computing method for set marginal density, it is still difficult to reach this goal for a universal RFS. The following results present a method to compute the set marginal density for a JMB-2 RFS.

Proposition 3: If Ψ is a JMB-2 RFS defined by its JMB-2 parameters $\{\epsilon_{10},\boldsymbol{\varrho}_{10},\epsilon_{01},\boldsymbol{\varrho}_{01},\epsilon_{11},\boldsymbol{\varrho}_{11}\}$, then Ψ is the union of two Bernoulli RFSs ψ_1, ψ_2. The set marginal density of ψ_i with respect to Ψ is a Bernoulli density with parameters $\{r_i, \mathbf{p}_i(\mathbf{x})\}, i = 1, 2$, where

$$\begin{aligned}
r_1 &= \epsilon_{10} + \epsilon_{11}\\
\mathbf{p}_1(\mathbf{x}) &= \frac{\epsilon_{10}}{\epsilon_{10}+\epsilon_{11}}\boldsymbol{\varrho}_{10}(\mathbf{x}) + \frac{\epsilon_{11}}{\epsilon_{10}+\epsilon_{11}}\int \boldsymbol{\varrho}_{11}((\mathbf{x},\mathbf{x}_2))d\mathbf{x}_2\\
r_2 &= \epsilon_{01} + \epsilon_{11}\\
\mathbf{p}_2(\mathbf{x}) &= \frac{\epsilon_{01}}{\epsilon_{01}+\epsilon_{11}}\boldsymbol{\varrho}_{01}(\mathbf{x}) + \frac{\epsilon_{11}}{\epsilon_{01}+\epsilon_{11}}\int \boldsymbol{\varrho}_{11}((\mathbf{x}_1,\mathbf{x}))d\mathbf{x}_1
\end{aligned} \tag{13}$$

Proof: Taking the set marginal density of ψ_1 for instance, due to the multi-hypotheses structure of Ψ, we can further represent $\Pr(\psi_1 \subseteq S, \Psi/\psi_1 \subseteq \mathbb{X})$ in (12) utilizing the whole probability formula:

$$\begin{aligned}
&\Pr(\psi_1 \subseteq S, \Psi/\psi_1 \subseteq \mathbb{X}) = \Pr(\psi_1 \subseteq S, \psi_2 \subseteq \mathbb{X})\\
&= \epsilon_{00} + \epsilon_{10}\Pr(\mathbf{x}_1 \in S | E_1 = 1, E_2 = 0)\\
&\quad + \epsilon_{01}\Pr(\mathbf{x}_2 \in \mathbb{X} | E_1 = 0, E_2 = 1)\\
&\quad + \epsilon_{11}\Pr((\mathbf{x}_1,\mathbf{x}_2) \in S \times \mathbb{X} | E_1 = 1, E_2 = 1)
\end{aligned} \tag{14}$$

Then using JMB-2 parameters, (14) can be further represented as:

$$\begin{aligned}
&\Pr(\psi_1 \subseteq S, \Psi/\psi_1 \subseteq \mathbb{X}) = \epsilon_{00} + \epsilon_{10}\int_S \boldsymbol{\varrho}_{10}(\mathbf{x})d\mathbf{x}\\
&+ \epsilon_{01} + \epsilon_{11}\int_{\mathbb{X}}\left(\int_S \boldsymbol{\varrho}_{11}((\mathbf{x}_1,\mathbf{x}_2))d\mathbf{x}_1\right)d\mathbf{x}_2
\end{aligned} \tag{15}$$

Based on *Proposition 2*, we can obtain set marginal density of ψ_1 with respect to Ψ by taking the set derivative of (15). In addition, the set density of ψ_2 can be computed as similar as ψ_1.

Remark: The *Definition 1*, *Proposition 2* provide a theoretical foundation to extract statistics of partial target states from global statistics in FISST framework. *Proposition 3* shows that it is convenient to compute the set marginal density of any random finite subset of a JMB-2 RFS by utilizing its JMB-2 parameters which incorporate the vector densities under different hypotheses.

D. Advantages of JMB-2 RFS

In this subsection, we summarize the advantages of JMB-2 RFS as follow:

1) *Each parameter within the JMB-2 parameters used to define a JMB-2 RFS has its own meaning and reveals some detail statistical information about the RFS, besides the global statistics of JMB-2 RFS.* One important aspect is that we can analyze the correlation between states in a JMB-2 RFS from two levels, i.e., $\rho_{E_1E_2}$ and $\boldsymbol{\rho}_{\mathbf{x}_1\mathbf{x}_2|H_{11}}$. Additionally, the probability about the existence of different targets, $\epsilon_{10}, \epsilon_{01}, \epsilon_{11}$, can also be achieved.

2) *The JMB-2 RFS family has a congenital advantage to extract the statistics of partial states from the global statistics.* A JMB-2 RFS is characterized by its JMB-2 parameters which incorporate vector densities under different hypotheses, and thus the defined marginal density of any subset of a JMB-2 RFS can be computed conveniently by utilizing the marginal density of random vector based on (13).

3) *The JMB-2 RFS family inherits advantages of the vector density in that the identities of target states are implicitly embedded with no need to augment target state with an extra label.* The JMB-2 RFS can be seen as the union of two Bernoulli RFSs with unknown level of correlation. As a Bernoulli RFS is used to describe a "twinkling" target, the index of Bernoulli RFS can be used to distinguish target identity. Moreover, the target labels implicit in the components of vector densities under different hypotheses are consistent with the indexes of Bernoulli RFSs.

Fig. 1 gives an example of JMB-2 parameters and the computing process of set marginal density for a JMB-2 RFS. It can be seen that the Bernoulli RFSs which construct this JMB-2 RFS are not independent. The corresponding correlation coefficient of E_1 and E_2, $\rho_{E_1E_2} = \frac{3}{8}$, based on (7). Under the hypothesis where two Bernoulli RFSs are not empty, the correlation coefficient between $x_1, x_2 \in R$, $\rho_{x_1x_2|H_{11}} = 0.8$.

IV. The Multi-target Filtering based on JMB-2 density

A. Problem Formulation

Suppose that at time k there are $n(k) \leq 2$ target states $\mathbf{x}_1^k, \ldots, \mathbf{x}_{n(k)}^k$, each taking values in a single target space $\mathbb{X}$, and $m(k)$ measurements $\mathbf{z}_1^k, \ldots, \mathbf{z}_{m(k)}^k$, each taking values in a measurement space $\mathbb{Z}$. The *multi-target state* and *multi-target measurement* at time k are represented as the finite

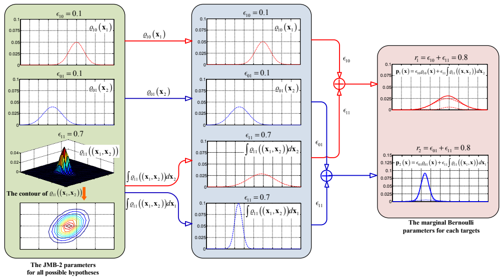

Fig. 1. Computing the set marginal density for a JMB-2 RFS.

sets, respectively, i.e., $X^k = \{\mathbf{x}_1^k, \ldots, \mathbf{x}_{n(k)}^k\}$ and $Z^k = \{\mathbf{z}_1^k, \ldots, \mathbf{z}_{m(k)}^k\}$.

The multi-target filtering problem can be cast as a multi-target Bayesian filter [9] on the space of finite sets $\mathcal{F}(\mathbb{X})$. The Bayesian filter propagates the posterior multi-target density $f(X^k|Z^{1:k})$ in time, which can be computed in two stages: prediction (16) and update (17).

$$f(X^k|Z^{1:k-1}) = \int f(X^k|X^{k-1}) f(X^{k-1}|Z^{1:k-1}) \delta X^{k-1} \tag{16}$$

$$f(X^k|Z^{1:k}) \propto g(Z^k|X^k) f(X^k|Z^{1:k-1}) \tag{17}$$

where $Z^{1:k}$ denotes the measurement history up to time k; $f(X^k|Z^{1:k-1})$ and $f(X^k|X^{k-1})$ denote multi-target predicted density and multi-target Markov transition density from time $k-1$ to k, respectively; $f(X^k|Z^k)$ and $g(Z^k|X^k)$ denote the multi-target posterior density and multi-target likelihood function at time k, respectively.

B. Target Dynamics and Measurement Model

We consider a "standard" multi-target motion model with no birth, which is similar to the case III in [9, Ch.13], for we only consider the case that the maximum cardinality is 2 in this paper. Given a multi-target state X^{k-1} at time k-1, each $\mathbf{x}^{k-1} \in X^{k-1}$ either survives into time step k with probability $p_S^k(\mathbf{x}^{k-1})$ and moves to a new state $\mathbf{x}^k$ with a Markov transition density $\mathbf{f}^{k|k-1}(\mathbf{x}^k|\mathbf{x}^{k-1})$, or dies with probability $1-p_S^k(\mathbf{x}^{k-1})$. Thus, the predicted multi-target state X^k conditioned on X^{k-1} at time k can represented as the union,

$$X^k = \bigcup_{\mathbf{x}^{k-1} \in X^{k-1}} \Upsilon(\mathbf{x}^{k-1}) \tag{18}$$

with $\Upsilon(\mathbf{x}^{k-1})$ the predicted state of $\mathbf{x}^{k-1}$. The motion and death of each targets are assumed to be conditional independent of the previous multi-target state X^{k-1}. The predicted multi-target state X^k is thus a multi-Bernoulli RFS conditioned on X^{k-1} with multi-Bernoulli parameters $\{p_S^k(\mathbf{x}^{k-1}), \mathbf{f}^{k|k-1}(\mathbf{x}^k|\mathbf{x}^{k-1})\}_{\mathbf{x}^{k-1}\in X^{k-1}}$. Additionally, we consider a generalized measurement model and the precise form of $g(Z^k|X^k)$ is not specified.

C. JMB-2 Filter

In this subsection, we show that the JMB-2 density permits an accurate closed-form solution under the prediction equation for a Markov transition model described in subsection IV-B and the update equation for a generalized multi-target likelihood function.

Proposition 4: Suppose that at time $k-1$, the posterior set density is a JMB-2 density with its JMB-2 parameters $\{\epsilon_{10}^{k-1}, \boldsymbol{\varrho}_{10}^{k-1}, \epsilon_{01}^{k-1}, \boldsymbol{\varrho}_{01}^{k-1}, \epsilon_{11}^{k-1}, \boldsymbol{\varrho}_{11}^{k-1}\}$, then under multi-target Markov transition model (18), the predicted set density is also a JMB-2 density with its JMB-2 parameters $\{\epsilon_{10}^{k|k-1}, \boldsymbol{\varrho}_{10}^{k|k-1}, \epsilon_{01}^{k|k-1}, \boldsymbol{\varrho}_{01}^{k|k-1}, \epsilon_{11}^{k|k-1}, \boldsymbol{\varrho}_{11}^{k|k-1}\}$, where

$$\begin{aligned}
\epsilon_{10}^{k|k-1} &= \epsilon_{10}^{k-1}\langle p_S^k, \boldsymbol{\varrho}_{10}^{k-1}\rangle_1 + \epsilon_{11}^{k-1}\langle p_S^k(\cdot)(1-p_S^k(\star)), \boldsymbol{\varrho}_{11}^{k-1}((\cdot,\star))\rangle_2 \\
\boldsymbol{\varrho}_{10}^{k|k-1}(\mathbf{x}_1^k) &= \frac{\epsilon_{10}^{k-1}}{\epsilon_{10}^{k-1|k}}\langle p_S^k \mathbf{f}^{k|k-1}(\mathbf{x}_1^k|\cdot), \boldsymbol{\varrho}_{10}^{k-1}\rangle_1 \\
&\quad + \frac{\epsilon_{11}^{k-1}}{\epsilon_{10}^{k-1|k}}\langle p_S^k(\cdot)(1-p_S^k(\star))\mathbf{f}^{k|k-1}(\mathbf{x}_1^k|\cdot), \boldsymbol{\varrho}_{11}^{k-1}((\cdot,\star))\rangle_2 \\
\epsilon_{01}^{k|k-1} &= \epsilon_{01}^{k-1}\langle p_S^k, \boldsymbol{\varrho}_{10}^{k-1}\rangle_1 + \epsilon_{11}^{k-1}\langle p_S^k(\star)(1-p_S^k(\cdot)), \boldsymbol{\varrho}_{11}^{k-1}((\cdot,\star))\rangle_2 \\
\boldsymbol{\varrho}_{01}^{k|k-1}(\mathbf{x}_2^k) &= \frac{\epsilon_{01}^{k-1}}{\epsilon_{01}^{k-1|k}}\langle p_S^k \mathbf{f}^{k|k-1}(\mathbf{x}_2^k|\cdot), \boldsymbol{\varrho}_{01}^{k-1}\rangle_1 \\
&\quad + \frac{\epsilon_{11}^{k-1}}{\epsilon_{01}^{k-1|k}}\langle p_S^k(\star)(1-p_S^k(\cdot))\mathbf{f}^{k|k-1}(\mathbf{x}_2^k|\star), \boldsymbol{\varrho}_{11}((\cdot,\star))\rangle_2 \\
\epsilon_{11}^{k|k-1} &= \epsilon_{11}^{k-1}\langle p_S^k(\cdot)p_S^k(\star), \boldsymbol{\varrho}_{11}^{k-1}((\cdot,\star))\rangle_2 \\
\boldsymbol{\varrho}_{11}^{k|k-1}((\mathbf{x}_1^k, \mathbf{x}_2^k)) &= \frac{\epsilon_{11}^{k-1}}{\epsilon_{11}^{k|k-1}} \\
&\quad \cdot \langle \mathbf{f}^{k|k-1}(\mathbf{x}_1^k|\cdot)\mathbf{f}^{k|k-1}(\mathbf{x}_2^k|\star), p_S^k(\cdot)p_S^k(\star)\boldsymbol{\varrho}_{11}^{k-1}((\cdot,\star))\rangle_2
\end{aligned} \tag{19}$$

Proposition 5: Suppose that at time k, the predicted set density is a JMB-2 density with its parameters $\{\epsilon_{10}^{k|k-1}, \boldsymbol{\varrho}_{10}^{k|k-1}, \epsilon_{01}^{k|k-1}, \boldsymbol{\varrho}_{01}^{k|k-1}, \epsilon_{11}^{k|k-1}, \boldsymbol{\varrho}_{11}^{k|k-1}\}$, then the updated set density is a JMB-2 density with its JMB-2 parameters $\{\epsilon_{10}^k, \boldsymbol{\varrho}_{10}^k, \epsilon_{01}^k, \boldsymbol{\varrho}_{01}^k, \epsilon_{11}^k, \boldsymbol{\varrho}_{11}^k\}$, where

$$\begin{aligned}
\epsilon_{10}^k &= \frac{\epsilon_{10}^{k|k-1}\langle g(Z^k|\{\cdot\}), \boldsymbol{\varrho}_{10}^{k|k-1}(\cdot)\rangle_1}{f^k(Z^k|Z^{1:k})} \\
\boldsymbol{\varrho}_{10}^k(\mathbf{x}^k) &= \frac{g(Z^k|\mathbf{x}^k)\boldsymbol{\varrho}_{10}^{k|k-1}(\mathbf{x}^k)}{\langle g(Z^k|\{\cdot\}), \boldsymbol{\varrho}_{10}^{k|k-1}(\cdot)\rangle_1} \\
\epsilon_{01}^k &= \frac{\epsilon_{01}^{k|k-1}\langle g(Z^k|\{\cdot\}), \boldsymbol{\varrho}_{01}^{k|k-1}(\cdot)\rangle_1}{f^k(Z^k|Z^{1:k})} \\
\boldsymbol{\varrho}_{01}^k(\mathbf{x}^k) &= \frac{g(Z^k|\{\mathbf{x}^k\})\boldsymbol{\varrho}_{01}^{k|k-1}(\mathbf{x}^k)}{\langle g(Z^k|\{\cdot\}), \boldsymbol{\varrho}_{01}^{k|k-1}(\cdot)\rangle_1} \\
\epsilon_{11}^k &= \frac{\epsilon_{11}^{k|k-1}\langle g(Z^k|\{\cdot,\star\}), \boldsymbol{\varrho}_{11}^{k|k-1}((\cdot,\star))\rangle_2}{f^k(Z^k|Z^{1:k})} \\
\boldsymbol{\varrho}_{11}^k(\mathbf{x}_1^k, \mathbf{x}_2^k) &= \frac{g(Z^k|\{\mathbf{x}_1^k, \mathbf{x}_2^k\})\boldsymbol{\varrho}_{11}^{k|k-1}((\mathbf{x}_1^k, \mathbf{x}_2^k))}{\langle g(Z^k|\{\cdot,\star\}), \boldsymbol{\varrho}_{11}^{k|k-1}(\cdot,\star)\rangle_2}
\end{aligned} \tag{20}$$

with

$$\begin{aligned}
f^k(Z^k|Z^{1:k}) = \epsilon_{00}^{k|k-1}g(Z^k|\emptyset) + \epsilon_{10}^{k|k-1}\langle g(Z^k|\{\cdot\}), \boldsymbol{\varrho}_{10}^{k|k-1}(\cdot)\rangle_1 \\
+ \epsilon_{01}^{k|k-1}\langle g(Z^k|\{\cdot\}), \boldsymbol{\varrho}_{01}^{k|k-1}(\cdot)\rangle_1 \\
+ \epsilon_{11}^{k|k-1}\langle g(Z^k|\{\cdot,\star\}), \boldsymbol{\varrho}_{11}^{k|k-1}((\cdot,\star))\rangle_2
\end{aligned} \tag{21}$$

Notice that under the hypothesis where both targets exist, as the measurement set Z^k does not provide any labelling information for targets, the labels of targets may become confusing when targets are in proximity. This phenomenon may lead to a multi-modal vector density $\boldsymbol{\varrho}_{11}^k((\mathbf{x}_1, \mathbf{x}_2))$. When this phenomenon arises, we can refer to the approach in [27] to switch a less multi-modal vector density, or the approach in [28] to build the track by minimising track jittering.

Propositions 4 and *5* imply that starting from a JMB-2 prior, all subsequent predicted and posterior densities are also JMB-2 densities. Multi-target Bayesian filter can be resolved in an accurate closed form when relevant densities are JMB-2 densities, which is referred to as the JMB-2 filter. A JMB-2 density is completely characterized by its JMB-2 parameters $\{\epsilon_{10}, \boldsymbol{\varrho}_{10}, \epsilon_{01}, \boldsymbol{\varrho}_{01}, \epsilon_{11}, \boldsymbol{\varrho}_{11}\}$, hence implementing the JMB-2 filter then amounts to recursively propagating JMB-2 parameters forward in time.

D. Multi-target State Extraction

Based on the advantages of the JMB-2 RFS in terms of computing set marginal density, a free-clustering state extraction approach is generated naturally for JMB-2 filter.

Firstly, compute the posterior set marginal densities for each "twinkling" targets by (13). The marginal densities of all "twinkling" targets can be represented as a group of Bernoulli parameters, i.e., $\{r_i^k, \mathbf{p}_i^k(\mathbf{x})\}_{i=1}^2$. r_i^k indicates how likely it is that hypothesized track i is a true target, and the posterior marginal density $\mathbf{p}_i^k(\mathbf{x})$ describes statistics of kinematics of the target i.

Secondly, compute the posterior cardinality distribution, estimate the number of targets as the expected or maximum a posteriori cardinality estimate, and select the corresponding number of the estimations from marginal densities ($\hat{\mathbf{x}}_i^k = \int_{\mathbb{X}} \mathbf{p}_i^k(\mathbf{x}) d\mathbf{x}$) with the highest existence probabilities r_i^k.

E. A correlation analysis method in tracking application

Based on the proposed state extraction method in subsection IV-D, another simple correlation analysis method suitable for the tracking scenario is proposed naturally. The targets 1 and 2 exhibit correlation, if $g(\hat{\mathbf{x}}_1^k, \hat{\mathbf{x}}_2^k) \leq \Lambda$, where Λ is a distance threshold, and $g(\cdot, \star)$ is a distance function depending on the way in which measurements are acquired. The similar method also has been used in [6], [7]. Compared with computing $\rho_{E_1 E_2}$ and $\boldsymbol{\rho}_{\mathbf{x}_1 \mathbf{x}_2 | H_{11}}$, this method can only provide a qualitative analysis about whether targets exhibit correlation or not, but it is a simple method and easy to realize. When the quantitative analysis is not required, this method is very meaningful.

V. Numerical Example

In this section, the advantages of JMB-2 RFS are verified by several numerical experiments. We consider a nonlinear superposition track-before-detect (TBD) measurement model for which PHD/CPHD and multi-Bernoulli filters [16] cannot obtain an accurate closed-form solution. Targets superposition on measurements are permitted when they are located in proximity. The surveillance region is divided into M cells. The measurement data at time k are collected in the vector $\mathbf{Z}^k = (\mathbf{z}_1^k, \cdots, \mathbf{z}_M^k) \in \mathbb{R}^M$, with $\mathbf{z}_j^k$ the intensity measurement obtained in the jth cell. The measurement set at time k is a singleton set, i.e., $Z^k = \{\mathbf{Z}^k\}$. The intensity measurements are assumed to be independently distributed conditioned on the multi-target state. The multi-target likelihood function can then be written as

$$g(Z^k | X^k) = \prod_{j=1}^{M} \ell(\mathbf{z}_j^k | X^k) \tag{22}$$

where $\ell(\mathbf{z}_j^k | X^k)$ is the measurement density for the jth cell. In the numerical examples a Gaussian model [31] is adopted:

$$\ell(\mathbf{z}_j^k | X^k) = \mathcal{N}(\mathbf{z}_j^k; \sum_{\mathbf{x} \in X^k} \sigma_j^T(\mathbf{x}), \sigma^N)$$

where $\sigma_j^T(\mathbf{x})$ is the power contribution from target state $\mathbf{x}$ to the jth cell and σ^N is noise power. Here, $\sigma_j^T(\mathbf{x})$ is described by a point spread function, for example,

$$\sigma_j^T(\mathbf{x}) = \frac{\delta_x \delta_y \sigma^T}{2\pi \sigma_b^2} \exp\left(-\frac{(\delta_x a - \theta_x)^2 + (\delta_y b - \theta_y)^2}{2\sigma_b^2}\right) \tag{23}$$

where σ^T is the source power, σ_b^2 is the blurring factor, and (θ_x, θ_y) is the position of target $\mathbf{x}$, δ_x and δ_y are cell side lengths, and $j = (a, b)$ denotes the position of jth cell in two-dimensionality image of the surveillance region. The SNR is defined by $10 \log(\sigma^T / \sigma^N)$.

In the following experiments, measurements are collected on a 230×60 grid with cell side lengths of $\delta_x = \delta_y = 1m$. We apply a point spread function with the blurring factor $\delta_b^2 = 1$. The SNR of each target is selected to be 15dB. The effective template $I(\mathbf{x})$ is the 5×5 pix square region whose center is closest to (θ_x, θ_y). The scenario involves two targets following a nonlinear nearly constant turn model [12], whose tracks cross twice, as shown in fig. 2. The number of total tracking frames is 96. Both targets are lasting from the 1st frame to the 96th frame.

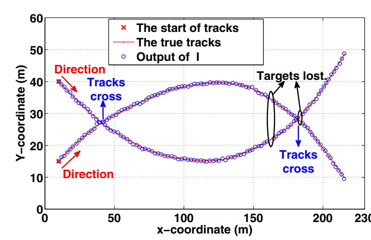

Fig. 2. Two targets whose tracks cross twice and the output of **I**.

A. Experiment 1

The implementation of JMB-2 filter is that $\boldsymbol{\varrho}_{10}^k(\mathbf{x})$, $\boldsymbol{\varrho}_{01}^k(\mathbf{x})$, and $\boldsymbol{\varrho}_{11}^k(\mathbf{x})$ are implemented using SMC approach with the particle number proportional to ϵ_{10}^k, ϵ_{01}^k and ϵ_{11}^k. In this experiment, the total number of particles is 100000. This object is to verify the first advantage of JMB-2 RFS mentioned in subsection III-E. Fig. 3 (a) shows the curves of $\epsilon_{01}^k, \epsilon_{10}^k, \epsilon_{11}^k$ over time for a single run. From Fig. 3 (a), it can be seen that during the whole scenario ϵ_{11}^k is extremely close to 1, which is consistence with that both true targets are surviving through the entire scenario. Hence, we omit the curve for the correlation coefficient $\rho_{E_1 E_2}^k$, and only analyze the correlation between target states under H_{11}. For convenience, we only provide one element of $\boldsymbol{\rho}^k_{\mathbf{x}_1^k\mathbf{x}_2^k|H_{11}}$, i.e., $\rho^k_{\theta^k_{x,1}\theta^k_{x,2}|H_{11}}$, the correlation coefficient between $\theta^k_{x,1}$ and $\theta^k_{x,2}$, with $\theta^k_{x,i}$ the position of $\mathbf{x}_i^k$ on x-coordinate, as shown in Fig. 3 (b). Another correlation analysis method for target tracking is also provided here. As the TBD styled measurements depend only on the targets positions, then a suitable distance function $g(\cdot,\star)$ is $|\hat{\boldsymbol{\theta}}_1^k - \hat{\boldsymbol{\theta}}_2^k|$, with $\hat{\boldsymbol{\theta}}_i^k$ the estimated position of target i. Fig. 3 (b) shows distance between the estimated targets position over time for a single run, and the distance threshold $\Lambda = 10m$. The two correlation analysis methods in Fig. 3 (b) both show that the correlation between posterior target states is extremely high when targets are in proximity, and is extremely low when targets are well separated. The reason is that when targets are closely spaced, target superpositions on measurements arise [6], [7] making the posterior target states not independent.

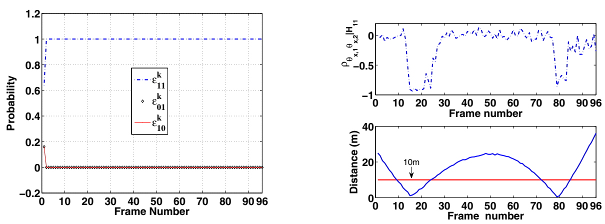

(a) (b)

Fig. 3. The curves of the some parameters over time: (a) the probabilities under different hypotheses, $\epsilon^k_{10}, \epsilon^k_{01}, \epsilon^k_{11}$, (b) the absolute correlation coefficient, $|\rho^k_{\theta_{x,1}\theta_{x,2}|H_{11}}|$.

B. Experiment 2

In this subsection, we assess the performance of three algorithms as follow:

I: The M-SMC filter [9] is given as benchmark with a common clustering approach, i.e., the Expectation Maximization (EM) algorithm [32] employed for multi-target state extraction. The particle number is set to be 1000. The M-SMC filter is chosen as benchmark for it is the only FISST based filter which can be closed form under any kind of measurement model, as it is the SMC approximation of optimal Bayesian filter.

II: The proposed JMB-2 filter is given. The total number of particles for $\boldsymbol{\varrho}^k_{10}(\mathbf{x}), \boldsymbol{\varrho}^k_{01}(\mathbf{x}), \boldsymbol{\varrho}^k_{11}(\mathbf{x})$ is 1000.

III: when targets are in proximity and may have correlation, JMB-2 filter which considers estimate targets jointly is employed. Then when the targets are far from each other and can be seen as posterior independence approximately, two parallel Bernoulli filters are employed. The transformation from JMB-2 filter to parallel Bernoulli filters is carried out through computing the posterior set marginal densities for each targets using (13) based on the correlation analysis. As we only require the information about whether targets have correlation, the method using the distance function in subsection IV-E is adopted and the threshold parameter is also set to be 10m. Due to this transformation, **III** can make full use of posterior independence while estimates targets jointly when they have correlation. For the JMB-2 filter, parameters are set as **II**. For the Bernoulli filter, the particle number for each $\mathbf{p}_i^k(\mathbf{x})$ is 1000.

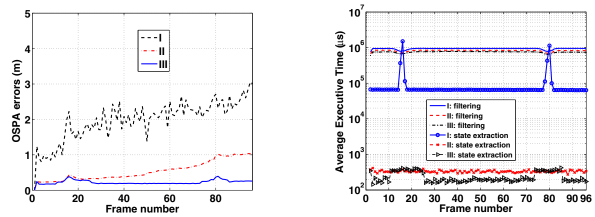

(a) (b)

Fig. 4. The performance metrics over time of I, II and III: (a) averaged OSPA errors, (b) averaged executive time.

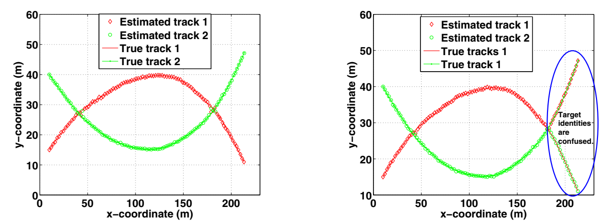

(a) (b)

Fig. 5. The estimated tracks for II: (a) case 1, (b) case 2.

For all the algorithms, track initiations are performed within the region around the true target states. The performance of three algorithms are examined in terms of the Optimal Sub-Pattern Assignment (OSPA) error [33] and the executive time. All performance metrics are averaged over 1000 independent Monte Carlo runs.

Fig. 4 (a) shows the estimation errors in terms of the averaged OSPA errors for **I**∼**III**. It can be seen that compare with **II** and **III**, **I** performs much more poorly, with the OSPA errors much higher and less stable. Fig. 2 also exhibits the output of **I** for a single run, which shows that sometimes targets are lost abnormally. The reason is that the clustering algorithm used to perform state extraction in **I** may bring the estimation deviation and is not very robust. Moreover, Fig. 4 (b) reflects that the average filtering time for **I**, **II** and **III** are at the same level, while the average executive time for states extraction of **I** is higher above 2.5∼4 orders of magnitude in terms of μs than the other two. Thus we conclude that the proposed free-clustering states extraction approach is much less burden-some, more accurate and robust than the clustering states extraction approach.

Fig. 4 (a) also demonstrates that performance improvement of **III** towards **II** is remarkable. The reason is that **III** can make full use of independence of two targets as soon as possible, and thus can achieve better performance than **III** for the same number of particles. In addition, Fig. 4 (b) also shows that the states extraction time for **III** is further reduced when transforming to the two parallel Bernoulli filters. We can conclude that after utilizing the advantage of first and second advantages of JMB-2 RFS, i.e., analyzing correlation between targets and extracting the statistics of the sub-set, the performance of the corresponding tracking filter can be further enhanced.

Additionally, Figs. 5 (a) and (b) show the estimated tracks built by **II** for two single runs respectively, which indicate that **II** has ability to identify the target identities and verify the third advantage of JMB-2 RFS. Actually, **III** also can build tracks, and for lack of space, we do not give here. It can be seen that the target identity can be recognized accurately when targets are well separated, however, when targets meet each other, target identities may be confused and will affect the remaining stage of tracking, as shown in Fig. 5 (b). Actually, the confusion of target identities when targets are in proximity is a common issue in multi-target tracking, and many scholars are devoted to study on this. The study on the track formation based on JMB-2 RFS, especially for closely spaced targets, is beyond the scope of this paper and will be done future.

VI. Conclusion

In this paper, we proposed a new class of RFS, joint multi-Bernoulli (JMB) RFS in the framework of random finite set (RFS), which is the union of a group of Bernoulli RFSs with unknown level of correlation, and is completely determined by a set of parameters. As a preliminary study, this paper provides both the derivations of the set density, set marginal density of the proposed RFS family, and the resultant tracking filter for a two-target scenario. The simulation results verify the advantages of the proposed JMB RFS family summarized in subsection III-E. Future works will expand the results of two-target scenario to multi-target scenario, i.e., JMB-N RFS. However, the JMB-N RFS suffers from problems that the number of hypotheses increases exponentially with the number of targets. The Efficient implementation with reasonable approximations for JMB-N filter will be studied in the future. Also the track formation based on JMB RFS especially for closely spaced targets also will be studied in the future.

References

[1] T. Fortmann, Y. Bar-Shalom, and M. Scheffe, "Sonar tracking of multiple targets using joint probabilistic data association," *IEEE J. Ocean. Eng.*, Vol. 8, No. 3, pp. 173-183, Jul. 1983.

[2] S. Deb, M. Yeddanapudi, K. Pattipati, and Y. Bar-Shalom, "A generalized s-d assignment algorithm for multisensor multitarget state estimation" *IEEE Trans. Aerosp. Electron. Syst.*, Vol. 33, No. 2, pp. 523-538, Apr. 1997.

[3] S. Blackman, "Multiple hypothesis tracking for multiple target tracking" *IEEE Aerosp. Electron. Syst. Mag.*, Vol. 19, No. 1, pp. 5-18, Jan. 2004.

[4] J. Vermaak, S. J. Godsill, and P. Perez, "Monte Carlo filtering for multi target tracking and data association," *IEEE Trans. Aerosp. Electron. Syst.*, Vol. 41, pp. 309-332, 2005.

[5] C. M. Kreucher, K. Kastella, and A. O. Hero, "Multi-target tracking using the joint multi-target probability density," *IEEE Trans. Aerosp. Electron. Syst.*, Vol. 41, No. 4, pp. 1396-1414, 2005.

[6] M. R. Morelande, C. M. Kreucher, and K. Kastella, "A Bayesian approach to multiple target detection and tracking," *IEEE Trans. on Signal Process.*, Vol. 55, No. 5, pp. 1598-1604, May 2007.

[7] W. Yi, M. R. Morelande, L. J. Kong, and J. Y. Yang, "A computationally efficient particle filter for multitarget tracking using an independence approximation," *IEEE Trans. on Signal Process.*, Vol. 61, No. 4, pp. 843-856, Feb. 2013.

[8] W. Yi, M. R. Morelande, L. J. Kong, and J. Y. Yang, "An efficient multi-frame track-Before-Detect algorithm for multi-target tracking", *IEEE J. Sel. Top. Signal Process.*, Vol. 7, No. 3, pp. 410-420, Jun. 2013.

[9] R. Mahler, Statistical multisource-multitarget information fusion, Norwood, MA: Artech House, 2007.

[10] R. Mahler, "'Statistics 101' for multisensor, multitarget data fusion," *IEEE Aerosp. Electron. Syst. Mag. part2: Tutorials*, Vol. 19, No. 1, pp. 53C64, Jan. 2004.

[11] R. Mahler, "'Statistics 102' multisource-multitarget detection and tracking", *IEEE J. Sel. Top. Signal Process.*, Vol. 7, No. 3, pp. 379-389, Jun. 2013.

[12] B. T. Vo and W. K.Ma, "The Gaussian mixture probability hypothesis density filter," *IEEE Trans. on Signal Process.*, Vol. 54, No. 11, pp. 4091-4104, Nov. 2006.

[13] B. T. Vo, B. N. Vo, and A. Cantoni, "The cardinality balanced multi-Target multi-Bernoulli filter and its implementations," *IEEE Trans. on Signal Process.*, Vol. 54, No. 11, pp. 4091-4104, Nov. 2006.

[14] B. N. Vo, S. Singh, and A. Doucet, "Sequential Monte Carlo methods for multi-target filtering with random finite sets," *IEEE Trans. Aersp. Electron. Syst.*, Vol. II, pp. 357-360, May. 2004.

[15] B. T. Vo, B. N. Vo and A. Cantoni, "The cardinality balanced multi-target multi-Bernoulli filter and its implementation," *IEEE Trans. on Signal Process.*, Vol. 57, No. 2, pp. 409-423, Feb. 2009.

[16] B. T. Vo, B. N. Vo, N. T. Pham and D. Suter, "Joint detection and estimation of multiple objects from image observation," *IEEE Trans. on Signal Process.*, Vol. 58, No. 10, pp. 5129-5141, Oct. 2010.

[17] B. Ristic, B. T. Vo, B. N. Vo and A. Farina, "A tutorial on Bernoulli filters: theory, implementation and applications," *IEEE Trans. Aersp. Electron. Syst.*, Vol. 61, No. 13, pp. 3406-3430, 2013.

[18] B. T. Vo and B. N. Vo, "Labeled random finite sets and multi-object conjugate priors," *IEEE Trans. on Signal Process.*, Vol. 61, No. 13, pp. 3460-3475, Jul. 2013.

[19] B. N. Vo, B. T. Vo, D. Phung, "Labeled random finite sets and the Bayes multi-target tracking filter," *IEEE Trans. on Signal Process.*, Vol. 62, No. 24, pp. 3460-3475, Dec. 2014.

[20] S. Reuter, B. T. Vo, B. N. Vo, and K. Dietmayer, "The labeled multi-bernoulli filter," *IEEE Trans. on Signal Process.*, Vol. 62, No. 12, pp. 3246-3240, Jun. 2014.

[21] F. Papi, B.-N. Vo, B.-T. Vo, C. Fantacci, and M. Beard,"Generalized Labeled Multi-Bernoulli Approximation of Multi-Object Densities," arXiv preprint, 2014, arXiv:1412.5294.

[22] C. Fantacci, B.-T. Vo, F. Papi, and B.-N. Vo,"The Marginalized δ-GLMB Filter" arXiv preprint arXiv:1501.00926, 2015.

[23] M. Beard, B.-T. Vo, and B.-N. Vo, "Bayesian Multi-target Tracking with Merged Measurements Using Labelled Random Finite Sets," Signal Processing, IEEE Transactions on, 2015.

[24] F. Papi and D.-Y. Kim, "A Particle Multi-Target Tracker for Superpositional Measurements using Labeled Random Finite Sets," arXiv preprint arXiv:1501.02248, 2014.

[25] Y. Bar-Shalom and E. Tse, "Tracking in a cluttered environment with probabilistic data association," *Automatica*, Vol. 11, No. 5, pp. 451C460, Sep. 1975.

[26] O. Kallenberg, Foundations of modern probability, MA: Artech House, 2002.

[27] L. Svensson, D. Svensson, M. Guerriero, and P. Willett, "Set JPDA filter for multitarget tracking," *IEEE Trans. on Signal Process.*, Vol. 59, No. 10, pp. 4677-4691, Oct. 2011.

[28] A. F. Garcła-Fernndez, M. R. Morelande and J. Grajal, "Bayesian sequential track formation," *IEEE Trans. on Signal Process.*, Vol. 62, No. 24, pp. 6366-6379, Oct. 2014.

[29] S. Q. Li, W. Yi, L. J. Kong, and B. L. Wang, "Dynamic factorization based multi-target Bayesian filter for multi-target detection and tracking", in *Proc. IEEE Int. Radar Conf.*, pp. 1251-1256, 2014.

[30] S. W. Shaw and J. F. Arnold, "Design and implementation of a fully automated oth radar tracking system," in *Rec. IEEE Int. Radar Conf.*, pp. 294-298, 1995.

[31] B. Ristic, S. Arulampalam, and N. J. Gordon, Beyond the Kalman filter: particle filters for tracking applications. Norwood, MA: Artech House, 2004.

[32] G. J. Mclachan and T. Krishnan, The EM algorithm and extensions, New York: John Wiley, 1975.

[33] D. Schumacher, B. T. Vo and B. N. Vo, "A consistent metric for performance evaluation of multi-object filters," *IEEE Trans. on Signal Process.*, Vol. 56, No. 8, pp. 3447-3457, Aug. 2008.